THE JOURNAL OF BIOLOGICAL CHEMISTRY VOL. 283, NO. 51, pp. 35772–35782, December 19, 2008

GBF1, a Transcription Factor of Blue Light Signaling in *Arabidopsis*, Is Degraded in the Dark by a Proteasome-mediated Pathway Independent of COP1 and SPA1*

Received for publication, May 6, 2008, and in revised form, October 10, 2008 Published, JBC Papers in Press, October 17, 2008, DOI 10.1074/jbc.M803437200

Chandrashekara Mallappa[1], **Aparna Singh**[1], **Hathi Ram**[1], **and Sudip Chattopadhyay**[2]

From the National Institute for Plant Genome Research, Laboratory 101, Aruna Asaf Ali Marg, New Delhi 110067, India

Arabidopsis **GBF1/ZBF2 is a bZIP transcription factor that plays dual but opposite regulatory roles in cryptochrome-mediated blue light signaling. Here, we show the genetic and molecular interrelation of GBF1 with two well characterized negative regulators of light signaling, COP1 and SPA1, in photomorphogenic growth and light-regulated gene expression. Our results further reveal that GBF1 protein is less abundant in the dark-grown seedlings and is degraded by a proteasome-mediated pathway independent of COP1 and SPA1. Furthermore, COP1 physically interacts with GBF1 and is required for the optimum accumulation of GBF1 protein in light-grown seedlings. Taken together, this study provides a mechanistic view of concerted function of three important regulators in *Arabidopsis* seedling development.**

Light is an important environmental factor for plant growth and development (1–3). Three distinct families of photoreceptors are involved in perception of various wavelengths of light: far-red and red light by phytochromes (phyA to phyE), blue and UV-A light by cryptochromes (cry1 to cry3) and phototropins (phot1 and phot2) (3–6). Recent studies demonstrate that, by altering the subcellular localization patterns, light controls the activity of photoreceptors. The cytosolic phytochromes are translocated into the nucleus upon light-mediated activation. Whereas cry2 is constitutively localized in the nucleus, cry1 is nuclear in the dark and is mostly cytoplasmic in the presence of light. cry3 has recently been shown to be transported into the chloroplast and mitochondria. Phototropins are mostly associated with the plasma membrane, and at least some fraction of phot1 is released into the cytoplasm upon light-mediated activation (7–10).

Significant progress has been made in recent years in understanding the functions of various downstream components in phytochrome signaling (1–3). However, similar information in cryptochrome-mediated blue light signaling is largely unknown (3, 5). Several regulatory proteins, including HY5, HYH, AtPP7, HFR1, SUB1, HRB1, OBP3, MYC2/ZBF1, and GBF1/ZBF2, have been reported to function in cryptochrome-mediated blue light signaling (11–19). Among these regulatory proteins, HYH, AtPP7, MYC2, and GBF1 are specifically involved in blue light-mediated photomorphogenic growth.

Photomorphogenesis is associated with several physiological responses that include: opening of apical hooks, expansion of cotyledons, inhibition of hypocotyl elongation, far-red light controlled blocking of greening, and accumulation of chlorophyll and anthocyanin (20–23). The expression of about one-third of the total genes in *Arabidopsis* is altered during the shift from skotomorphogenic to photomorphogenic growth (24, 25). COP1 acts as an ubiquitin ligase and helps to degrade the photomorphogenesis-promoting factors such as HY5, HYH, LAF1, and HFR1 in the dark (15, 26–30). The *cop1* mutant seedlings show photomorphogenic growth in darkness, hypersensitive responses to light and less lateral roots as compared with wild-type plants (31, 32). Recent studies have shown that COP1 interacts with SPA1, and this interaction modulates the proteasome-mediated degradation of HY5, HFR1, and LAF1 (33–37). SPA1 was originally isolated as a negative regulator of far-red light signaling. The *spa1* mutants are hypersensitive to far-red light, red light, and blue light (33, 38, 39).

A group of bZIP transcription factors (GBFs)[3] has been isolated that can specifically interact with the G-box, one of the four light-responsive elements commonly found in the light-regulated promoters (40–45). The subcellular localization studies indicate that the light-controlled nuclear translocation is one of the important mechanisms for the activities of GBFs (46). However, the specific functions of most these genes *in vivo* have yet to be defined. Recently, GBF1/ZBF2 has been identified in a Southwestern screen using the Z-box light-responsive element as ligand (19). The investigation of physiological functions of GBF1 has revealed that it functions in cryptochrome-mediated blue light signaling and plays a dual but opposite regulatory role in *Arabidopsis* seedling development (19). In this study, we show the functional relationships of GBF1 with two well-characterized negative regulators of light signaling, COP1 and SPA1, in *Arabidopsis* seedling development.

EXPERIMENTAL PROCEDURES

Plant Materials, Growth Conditions, and Generation of Double Mutants—Surface-sterilized seeds of *Arabidopsis thaliana* were sown on MS plates, stratified at 4 °C in darkness for 3–5

* This work is supported in part by a Ramanna Fellowship grant from the Dept. of Science and Technology, Government of India (to S. C.). The costs of publication of this article were defrayed in part by the payment of page charges. This article must therefore be hereby marked "*advertisement*" in accordance with 18 U.S.C. Section 1734 solely to indicate this fact.

[1] Recipients of Council of Scientific and Industrial Research/University Grants Commission fellowships, Government of India.

[2] To whom correspondence should be addressed. Tel.: 91-11-2673-5175; Fax: 91-11-2674-1658; E-mail: sudipchatto@yahoo.com.

[3] The abbreviations used are: GBF1, G-box binding factor 1; ZBF2, Z-box binding factor 2; bZIP, basic leucine zipper; GST, glutathione *S*-transferase; WL, white light; D, dark; FR, far-red light; RL, red light; BL, blue light; E3, ubiquitin-protein isopeptide ligase.

days, and transferred to specific light conditions at 22 °C. The *Arabidopsis* growth conditions and the intensities of continuous light sources used in this study have been described in a previous study (18). For the generation of double mutants, such as *gbf1-1 cop1-4*, *gbf1-1 cop1-6*, or *gbf1-1 spa1-1* homozygous *gbf1-1* mutant plants were crossed individually with *cop1-4*, *cop1-6*, or *spa1-1* homozygous mutant lines. In F2 generation, seedlings were grown in WL (60 mmol m^{-2} s^{-1}) for the identification of *cop1-4* or *cop1-6* homozygous lines, or FR (40 mmol m^{-2} s^{-1}) for *spa1-1* homozygous lines, and seedlings with typical short hypocotyls phenotype of *cop1* mutants were selected and transferred to soil. For *spa1*, seedlings were kept in WL for 2 days and then short hypocotyls phenotype spa1 mutants were transferred to soil. To determine the genotype at *gbf1* locus, ~40 seedlings from each line were tested by genomic PCR. F3 progeny that are homozygous for *gbf1-1* mutant plants were further examined and considered as *gbf1 cop1-4*, *gbf1 cop1-6*, or *gbf1 spa1* double mutants. Blocking of greening phenotype of *cop1* and *gbf1 cop1* was done as described before (47). Root growth and flowering phenotype experiments were carried out essentially as described (19). FR-mediated blocking of greening phenotype was carried out as described (33).

For 26 S proteasome inhibitors (MG132, MG115, and *N*-acetyl-leucyl-leucyl-norleucinal) and DMSO treatments, the seedlings were grown under required light conditions (as mentioned in the figure legends) and then seedlings were collected by forceps and incubated in liquid MS medium (Sigma) containing proteasome inhibitor (50 μM dissolved in DMSO) or containing 0.1% DMSO under required conditions as indicated in text for 12 h. At the end of the incubation, the seedlings were thoroughly washed with liquid MS medium three times to remove residual proteasome inhibitor or DMSO, and the seedlings were either incubated in liquid MS medium for different time points as indicated in text or frozen in liquid nitrogen for total protein extraction.

Affinity Purification of GBF1 Antibody—The antibody of GBF1 was raised against N-terminal GBF1 protein (from 1 to 172 amino acids) by Bangalore GeneI, Bangalore, India. The steps of affinity purification of antibodies are given below.

Ligand coupling: 2–3 mg of 6× His-ΔN-ZBF2 protein was dialyzed against 13% polyethylene glycol 8000 in coupling buffer (0.2 M $NaHCO_3$, 0.5 M NaCl, pH 8.3) to concentrate to 1 ml. The top cap of the NHS-HP column was removed, and a drop of ice-cold 1 mM HCl was added to avoid air bubbles. A Hi-Trap adaptor was connected to the top of the column. Isopropanol in the column was washed with ice-cold 1 mM HCl with a flow rate of 1 ml/min. Immediately afterward, 1 ml of ligand solution was injected into the column, and the column was left to stand for 4 h at 4 °C. Any excess active groups not coupled to the ligand were deactivated and washed out by washing with Buffer A (0.5 M ethanolamine, 0.5 M NaCl, pH 8.3) and Buffer B (0.1 M sodium acetate, 0.5 M NaCl, pH 4.0). Finally, 2 ml of phosphate-buffered saline buffer with neutral pH was injected.

Antibody purification: A blank run was performed before the experiment to ensure loosely bound ligand is washed off. The column was prepared by washing with 3 ml of start buffer (phosphate-buffered saline) and 3 ml of elution buffer (100 mM glycine, pH 2.5). The column was equilibrated with 10 column volumes of start buffer. Antibody sample was adjusted to the composition of start buffer. This was done by diluting the sample with start buffer. The sample was filtered through a 0.45 μm filter before it was applied to the column. Antibody sample was applied using a syringe fitted to luer adaptor. A flow rate of 0.2–1 ml/min was maintained. The column was incubated for 4–6 h in a cold room. Then the column was washed with 5–10 column volumes of start buffer, until no material was left in the effluent. Antibody was eluted with 1–3 ml of elution buffer. Column was re-equilibrated by washing with 5–10 column volumes of start buffer. Column is stored in storage buffer (0.05 M sodium phosphate buffer, 0.1% sodium azide, pH 7.0).

Total Protein Extraction from Arabidopsis—The seedlings (100 mg) were frozen in liquid nitrogen and ground in 300 μl of grinding buffer (400 mM sucrose, 50 mM Tris-Cl, pH 7.5, 10% glycerol, 2.5 mM EDTA), and phenylmethylsulfonyl fluoride was added (0.5 μl for every 100 μl of grinding buffer). The protein extract was transferred to fresh microcentrifuge tube and centrifuged at 5000 rpm for 5 min to pellet down the debris. The supernatant was transferred to a fresh tube, and an aliquot of 5 μl was taken out in a separate tube for the estimation of protein by Bradford assay. To the rest of the protein extract, appropriate volume of 4× sample buffer (200 mM Tris-Cl, pH 6.8, 400 mM dithiothreitol, 4% SDS, 0.025% Bromphenol Blue, 20% glycerol), *i.e.* 1/4th of grinding buffer = volume of 4× sample buffer, was added and boiled for 5 min before loading on SDS-PAGE.

Western Blot Analysis—Western blotting was performed using the SuperSignal West Pico chemiluminescent substrate kit (Pierce) and following the instructions as described in the user's manual provided by the manufacturer. The samples were then run on SDS-PAGE gel and transferred to Hybond ECL nitrocellulose membrane (GE Healthcare) at 100 mA for 2 h in transfer buffer (Tris (7.56 g), glycine (47 g), 20% methanol in 2.5 liters) in Mini blot protein gel apparatus (GE Healthcare). 40 μg of total protein was used for Western blot analysis. The membrane was stained with Ponceau-S to confirm the protein transfer and washed with sterile milli-Q water. The membrane was then incubated for 1 h in 2 ml of blocking buffer (5% nonfat dry milk in Tris-buffered saline and 0.05% Tween 20) at room temperature with shaking. The blocking reagent was removed, and the affinity-purified primary antibody diluted (1:300 to 1:500) in 15 ml of blocking buffer with 0.05% Tween 20 was added and incubated for 2 h with shaking at room temperature. The membrane was then washed with 15 ml of wash buffer (Tris-buffered saline and 0.05% Tween 20) for thrice, 5 min each. The secondary antibody, conjugated with horseradish peroxidase diluted (1:20,000) in 15 ml of blocking buffer with 0.05% Tween 20, was added and incubated for 1 h with shaking at room temperature. The membrane was washed with 15 ml of wash buffer for five times at room temperature. The working solution of substrate was prepared by mixing peroxide solution and luminol/enhancer solution in 1:1 ratio, and the blot was incubated in that working solution for 5 min in darkness. The blot was then removed from the working solution and covered with plastic wrap in a cassette and exposed to x-ray film for different times.

The actin band probed with anti-actin (Catalog no. A0A80, Sigma) antibodies was used as a loading control.

Protein-Protein Interaction Studies—In vitro binding assay: GST and GST-GBF1 fusion proteins were expressed in *Escherichia coli* strain (BL21/DE3) and purified using glutathione-agarose beads (GE Healthcare) as described (18). About 5 mg of GST or GST-GBF1 was bound to the glutathione-Sepharose 4B beads by incubating for 2 h at 4 °C. Beads were washed and incubated with COP1–6His (5 mg) for overnight at 4 °C. Beads were washed thrice with the binding buffer, boiled with the loading dye, and loaded onto the SDS-PAGE. The blot was probed with anti-COP1 antibodies. To generate constructs for yeast two-hybrid assays, full-length *GBF1* and *HY5* were cloned into pGADT7 vector with ECOR1-BamH1 and Nde1-Cla1 restriction sites, respectively, to produce translational fusions with the activation domain. To generate DBD-COP1, an EcoR1-Pst1 PCR fragment of full-length *COP1* was cloned into the corresponding sites of the vector pGBKT7 (Clontech) to produce translational fusion with DNA binding domain. The constructs were transformed into Yeast strain AH109 according to the Clontech protocol. Expression of AD-GBF1 and AD-HY5 fusion proteins were examined by hemagglutinin and DBD-COP1 by c-Myc antibodies. The protein-protein interactions were examined by β-galactosidase assays. The relative β-galactosidase activities were calculated according to Clontech instructions. *In vitro* The coimmunoprecipitation experiment was as follows: ~5 mg of anti-GST antibodies was bound to protein A-agarose beads by incubating for 6 h at 4 °C. After washing the beads bound to the antibodies, GST-GBF1 and COP1–6His proteins were added and incubated for overnight at 4 °C in a 250-ml reaction volume. Beads (pellet) were washed thrice with the binding buffer, boiled with the loading dye, and loaded separately along with the supernatant onto SDS-PAGE. The blot was probed with anti-COP1 antibodies.

Chlorophyll and Anthocyanin Measurements—Chlorophyll and anthocyanin levels were measured following protocols as described in a previous study (15).

Quantitative Real-time PCR Analyses—Wild-type and different mutant seedlings were grown under required conditions. Total RNA was extracted from seedlings at different time points using an RNeasy Plant Mini Kit (Qiagen), and cDNA were synthesized from total RNA using a Titan One Tube RT-PCR system (Roche Applied Science) following the manufacturer's instructions. Real-time PCR analyses of gene expression were carried out by using LightCycler® FastStart DNA Master^{PLUS} SYBR Green I (Roche Applied Science) and LightCycler® 2.0 system (Roche Applied Science). Primer sequences used for PCR amplification of *CAB1* were 5′-CCCATTTCTTGGCTTACAACAAC-3′ and 5′-TCGGGGTCAGCTGAAAGTCCG-3′; primers for *RBCS-1A* were 5′-GAGTCACACAAAGAGTAAAGAAG-3′ and 5′-CTTAGCCAATTCGGAATCGGT-3′; primers for *ADH1* were 5′-CCGAAAGACCATGACAAGCCAA-3′ and 5′-GATGCAACGAATACTCTCTCCC-3′; primers for *ACTIN2* were 5′-GCCATCCAAGCTGTTCTCTC-3′ and 5′-GCTCGTAGTCAACAGCAACAA-3′. The transcript levels are normalized to the level of *ACTIN2* transcript abundance.

RESULTS

The Photomorphogenic Growth of cop1 Mutants in Dark Is Enhanced in gbf1 cop1 Double Mutants—Acting as an E3 ubiquitin ligase, COP1 helps to degrade or stabilize several regulatory proteins in darkness and thereby suppresses photomorphogenesis. The *cop1* mutants display photomorphogenic growth in the dark and hypersensitive responses to various wavelengths of light. We ask whether the BL-specific transcription factor, GBF1, which plays both positive and negative regulatory roles in light signaling, is functionally related to COP1. Among the various alleles of *cop1* mutants identified and characterized, *cop1-4* and *cop1-6* mutants are relatively weak alleles, and *cop1-6* mutants display shorter hypocotyl than *cop1-4* in the darkness. Because the null alleles of *cop1* are seedling-lethal, we chose *cop1-4* and *cop1-6* mutants for our studies. Whereas *cop1-4* encodes a truncated COP1 terminated at amino acid 282, *cop1-6* allele contains an in-frame five-amino acid insertion between codons 301 and 302.

To determine the genetic interactions between *COP1* and *GBF1*, we constructed *gbf1-1 cop1-4* and *gbf1-1 cop1-6* double mutants and investigated the morphology of the double mutants in darkness and various light conditions. Although *gbf1* seedlings did not exhibit any altered morphology in darkness, *gbf1 cop1* double mutants exhibited shorter hypocotyl than *cop1* mutants, suggesting that *gbf1* and *cop1* function synergistically in repressing photomorphogenic growth in the darkness (Fig. 1*A*). We then examined the growth of 6-day-old *gbf1 cop1* double mutants under various light conditions, including red light (RL), far-red light (FR), and blue light (BL). The *gbf1 cop1* double mutants were significantly shorter than *cop1* or *gbf1* single mutants in BL (Fig. 1*B*), indicating an additive effect of *gbf1* and *cop1* mutations on BL-mediated inhibition of hypocotyl elongation. However, in WL (white light), RL, or FR, *gbf1 cop1* seedlings were morphologically indistinguishable from *cop1* single mutants, suggesting that *cop1* is epistatic to *gbf1* in WL-, RL-, or FR-mediated inhibition of hypocotyl elongation (Fig. 1, *C–E*).

Although GBF1 plays a negative regulatory role in BL-mediated inhibition of hypocotyl elongation, it acts as a positive regulator of cotyledon expansion. The cotyledons of *gbf1* mutants are less expanded compared with corresponding wild-type seedlings (19). The BL-grown *cop1-4* mutant seedlings have more expanded cotyledons than wild type, however this effect is less prominent in *cop1-6* mutant seedlings. Examination of the cotyledon size revealed that *gbf1 cop1* double mutants have cotyledon size similar to wild-type seedlings suggesting that GBF1 and COP1 function antagonistically in regulating the BL-mediated cotyledon expansion (Fig. 1*F*).

The Fusca and Blocking of Greening Phenotypes of cop1 Are Further Enhanced in gbf1 cop1 Double Mutants—The *cop1* mutants display dark purple color fusca phenotype due to high level accumulation of anthocyanin, however such effects are not visible in *gbf1* mutants. The number of fusca phenotype, when examined, was dramatically increased in *gbf1 cop1* double mutants as compared with *cop1* single mutants. Although the effect was only visible in *gbf1 cop1-6* double mutants at lower fluence rates of WL, both *gbf1 cop1-4* and *gbf1 cop1-6* double

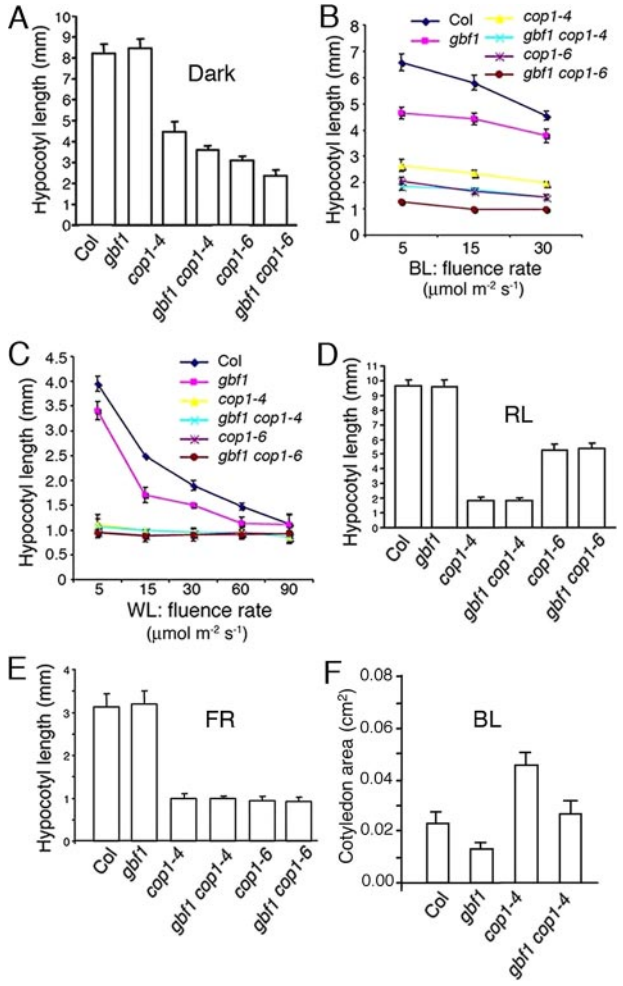

FIGURE 1. **Analyses of *gbf1 cop1* double mutants.** 25–30 seedlings were used for the measurement of hypocotyl length. The *error bars* indicate standard deviation in this and all subsequent figures unless otherwise mentioned. *A*, hypocotyl length of 6-day-old wild-type (*Col*) and different mutant seedlings grown in constant darkness. *B*, hypocotyl length of 6-day-old wild-type (*Col*) and different mutant seedlings grown at various fluences of blue light (*BL*). *C*, hypocotyl length of 6-day-old wild-type (*Col*) and different mutant seedlings grown at various fluences of white light (*WL*). *D*, hypocotyl length of 6-day-old wild-type (*Col*) and different mutant seedlings grown in red light (RL: 60 μmol m^{-2} s^{-1}). *E*, hypocotyl length of 6-day-old wild-type (*Col*) and different mutant seedlings grown in far-red light (FR: 40 μmol m^{-2} s^{-1}). *F*, cotyledon area of 6-day-old seedlings grown in blue light (BL: 20 μmol m^{-2} s^{-1}).

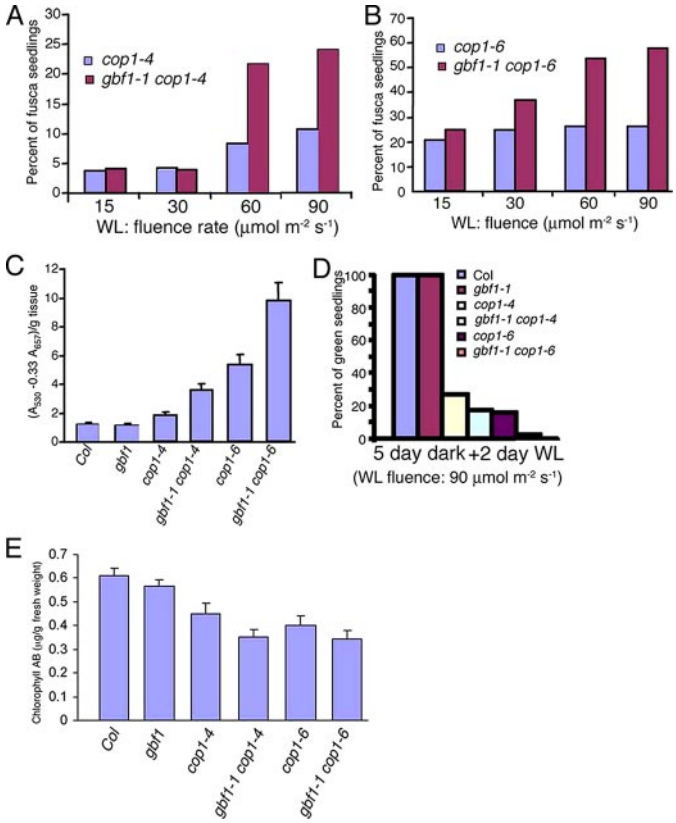

FIGURE 2. **Physiological properties of *gbf1 cop1* double mutants.** *A* and *B*, percentage of fusca phenotype in 6-day-old seedlings grown at various fluences of WL. *C*, accumulation of anthocyanin in 6-day-old seedlings grown in WL (90 μmol m^{-2} s^{-1}). *D*, percentage of seedlings turned green while 5-day-old dark-grown seedlings were transferred to WL for 2 days. *E*, accumulation of chlorophyll in 6-day-old seedlings grown in WL (90 μmol m^{-2} s^{-1}).

mutants displayed higher percentage of fusca phenotype at higher intensity of WL (Fig. 2, *A* and *B*). Consistent with this observation, the quantification of anthocyanin levels revealed an increase in anthocyanin accumulation in *gbf1 cop1* double mutants as compared with *cop1* alone (Fig. 2*C*).

The dark-grown *cop1* mutants are sensitive to high intensity light, and some of them do not turn green when transferred to light. The COP1-mediated blocking of greening phenotype becomes more intense with longer incubation in the darkness (47). We examined the blocking of greening effects in *gbf1 cop1* double mutants. A lower percentage of *gbf1 cop1* double mutants than *cop1* alone were able to turn green when 5-day-old dark-grown seedlings were transferred to light (Fig. 2*D*), suggesting that *gbf1* can enhance the blocking of greening phenotype of *cop1*. Examination of chlorophyll contents reveals that the chlorophyll content of *gbf1 cop1* double mutants was lower than either of the single mutants (Fig. 2*E*).

The Altered Root Growth and Flowering Time of cop1 Mutants Are Enhanced by Additional Loss of Function of GBF1—Both *cop1* and *gbf1* plants show less number of lateral roots compared with wild-type plants, although the effect is more pronounced in *cop1* mutants. To determine the genetic relationships between *cop1* and *gbf1* mutant plants in lateral root formation, we examined the root growth of 16-day-old *gbf1 cop1* double mutants and compared with *cop1* or *gbf1* single mutants. As shown in Fig. 3*A*, *gbf1 cop1* double mutants developed fewer lateral roots compared with *gbf1* or *cop1* single mutants. There was hardly any lateral root visible in *gbf1 cop1-6* double mutants up to 16 days. Mutations in *GBF1* or *COP1* result in early flowering under long day conditions. Examination of flowering time in *gbf1 cop1* double mutants revealed that the early flowering phenotype of *gbf1* is significantly ($p < 0.02$) enhanced in *gbf1 cop1* double mutant background under long day conditions (Fig. 3*B*).

GBF1 and SPA1 Act in an Independent and Interdependent Manner in BL-mediated Photomorphogenic Growth—The light-specific negative regulator, SPA1, has been shown to be functionally associated with COP1 in degradation of photomorphogenesis-promoting factors in the dark. The loss-of-function mutants of *SPA1* do not show any morphological defects in the darkness; however, *spa1* mutants show hypersensitive response to far-red, red, and blue light. Three alleles of

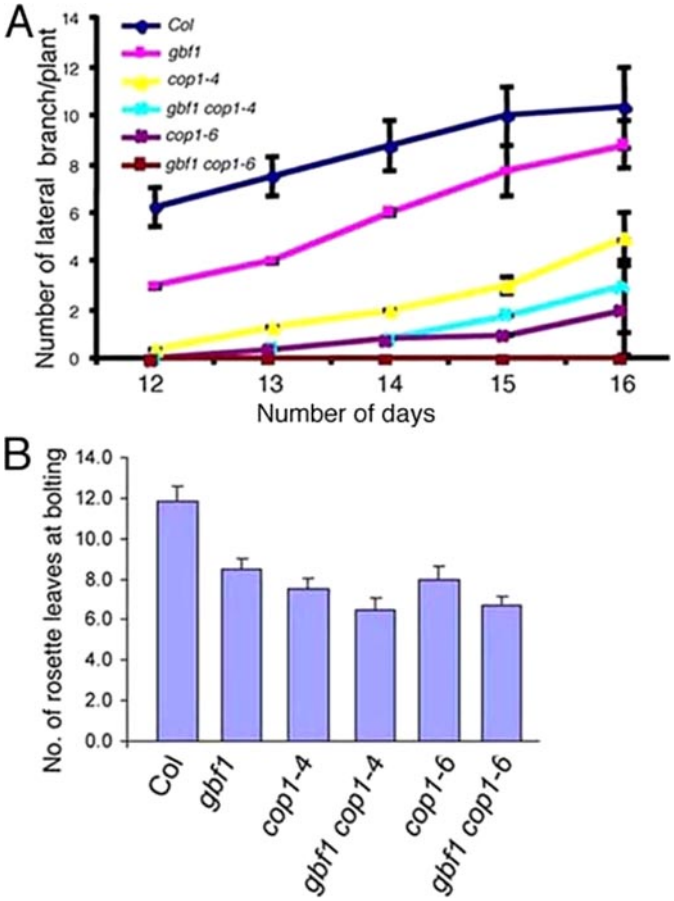

FIGURE 3. **Characterization of *gbf1 cop1* adult plants.** *A*, number of lateral roots formed in 16-day-old wild-type (*Col*) and various mutant plants grown under constant WL (100 μmol m^{-2} s^{-1}). *B*, number of rosette leaves formed at the time of bolting in wild-type (*Col*) and different mutants plants grown under long day conditions of 14-h WL (100 μmol m^{-2} s^{-1}) and 10-h dark cycles.

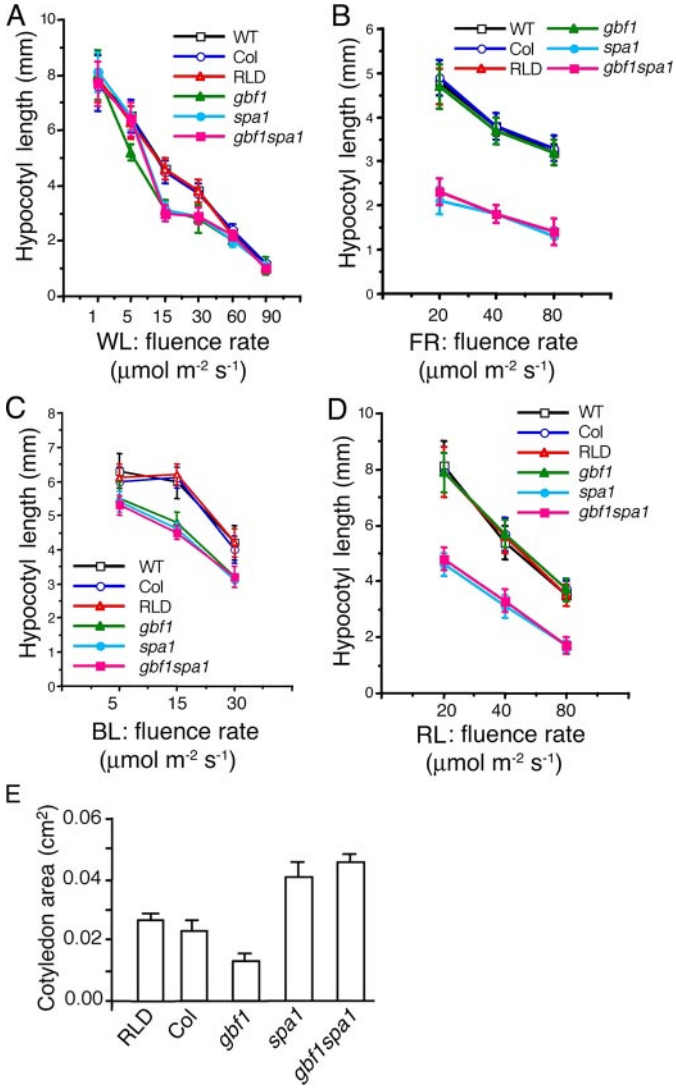

FIGURE 4. **Analyses of *gbf1 spa1* double mutants.** 25–30 seedlings were used for the measurement of hypocotyl length. *A–D*, hypocotyl length of 6-day-old Col, RLD ecotype, segregated wild-type (WT) and different mutant seedlings grown at various fluences of WL, FR, BL and RL, respectively. *E*, cotyledon area of 6-day-old seedlings grown in blue light (20 μmol m^{-2} s^{-1}).

spa1 mutant were originally identified, which showed similar morphological defects. Among these, in *spa1-1* mutants, *SPA1* carries a single base pair substitution resulting in a stop codon, and thereby produces a 848-amino acid truncated protein. Because analyses of *gbf1 cop1* double mutants reveal functional interrelation between *GBF1* and *COP1*, we ask whether *GBF1* is also functionally connected to *SPA1*.

To examine possible genetic interactions between *gbf1* and *spa1*, we constructed *gbf1-1 spa1-1* double mutants and examined their growth in darkness and various light conditions. The dark-grown *gbf1 spa1* double mutant seedlings showed wild-type phenotype, similar to *gbf1* or *spa1* single mutants. In WL and BL, the enhanced inhibition of hypocotyl elongation caused by *gbf1* mutations was found to be similar to *spa1*. The *gbf1 spa1* double mutants displayed hypocotyl length similar to *gbf1* or *spa1* single mutants, suggesting that *gbf1* and *spa1* act independently in WL- and BL-mediated inhibition of hypocotyl elongation (Fig. 4, *A* and *C*). However, under RL or FR, *gbf1 spa1* double mutants showed similar hypocotyl lengths to *spa1*, suggesting *spa1* is epistatic to *gbf1* in RL- or FR-mediated inhibition of hypocotyl elongation (Fig. 4, *B* and *D*). Similar to *cop1* mutants, *spa1* mutants also display more expanded cotyledons in BL. The cotyledon size of *gbf1 spa1* double mutants was found to be similar to *spa1* in BL, suggesting that *spa1* is epistatic to *gbf1* in BL-mediated cotyledon expansion (Fig. 4*E*).

Genetic Interactions between GBF1 and SPA1 Modulate Physiological Responses and Root Growth—When grown in RL and FR, *spa1* mutants accumulate higher levels of anthocyanin than wild-type seedlings. Although *gbf1* mutants do not display significant difference in anthocyanin accumulation as compared with wild type, the anthocyanin content of *gbf1 spa1* double mutants was drastically increased as compared with corresponding single mutants in BL (Fig. 5*A*). On the other hand, accumulation of anthocyanin in *gbf1 spa1* double mutants was found to be similar to *spa1* alone in WL and FR (Fig. 5, *B* and *C*). Pre-exposure to FR of *Arabidopsis* seedlings prevent greening when seedlings are subsequently exposed to WL. To determine the FR-mediated blocking of greening effect in *gbf1 spa1* double mutants, we grew the seedlings in FR for 3 days and then transferred them to white light. Whereas *gbf1* or *spa1* mutant seedlings showed ~20–80% of pale green phenotype with no visible

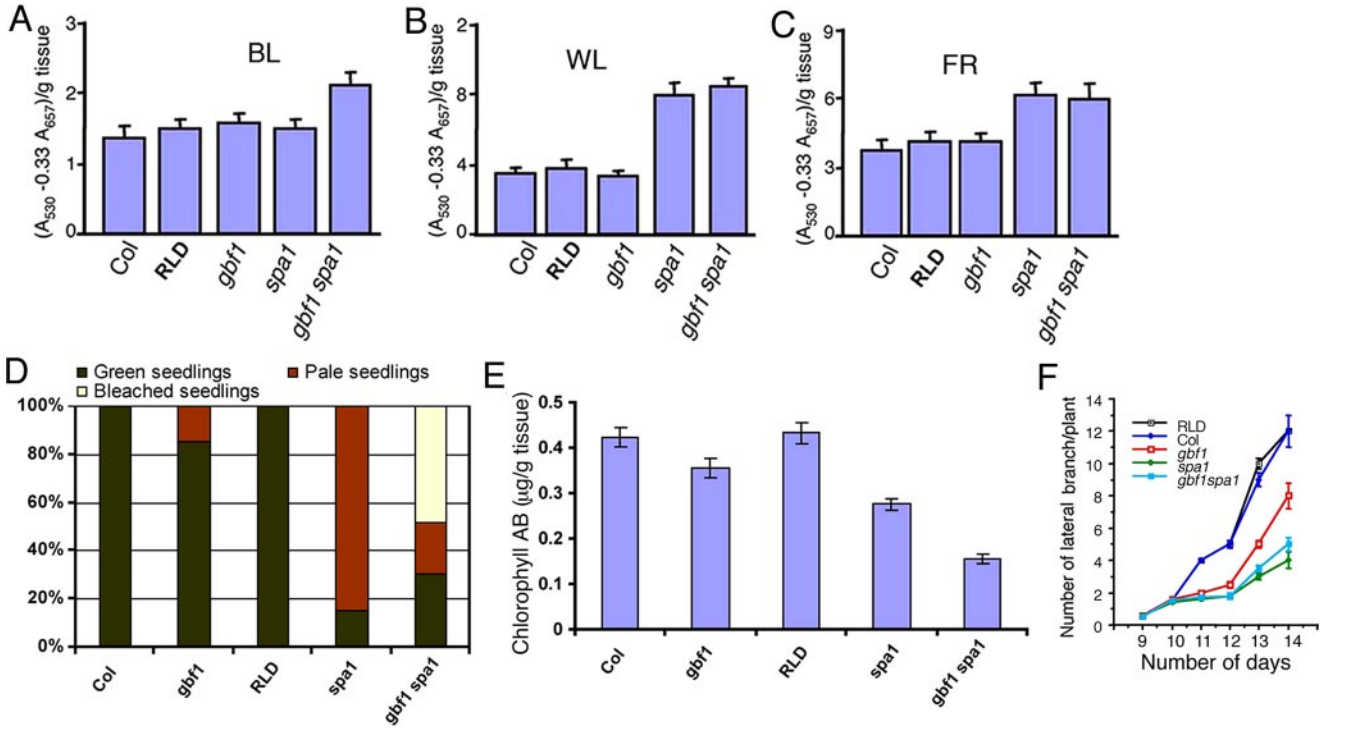

FIGURE 5. **Physiological properties and root growth of *gbf1 spa1* double mutants.** *A–C*, accumulation of anthocyanin in 6-day-old seedlings grown in BL (30 μmol m^{-2} s^{-1}), WL (90 μmol m^{-2} s^{-1}), or FR (80 μmol m^{-2} s^{-1}), respectively. *D*, quantification of the number of seedlings turned green while 3-day-old seedlings grown in FR (40 μmol m^{-2} s^{-1}) were transferred to WL (90 μmol m^{-2} s^{-1}) for 2 days. *E*, accumulation of chlorophyll in 3-day-old FR (40 μmol m^{-2} s^{-1})-grown seedlings transferred to WL (90 μmol m^{-2} s^{-1}) for 2 days. *F*, the number of lateral roots formed in wild-type (*Col*) and various mutants grown in WL (100 μmol m^{-2} s^{-1}) at different days.

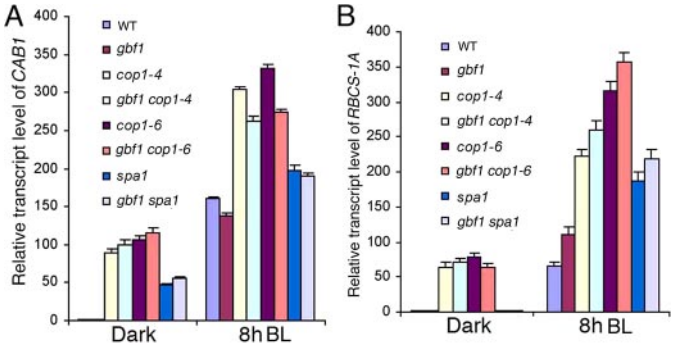

FIGURE 6. **Expression of *CAB1* and *RBCS-1A* in *gbf1 cop1* and *gbf1 spa1* double mutants.** *A*, the abundance of *CAB1* transcripts in total RNA from wild-type and different mutant seedlings grown in darkness for 5 days and transferred to BL (20 μmol m^{-2} s^{-1}) for 8 h was determined by quantitative real-time PCR, and the transcript levels were normalized to the level of *ACTIN2* transcript abundance. *B*, the abundance of *RBCS-1A* transcripts determined by quantitative real time PCR as described in *A*.

bleaching effects, >40% *gbf1 spa1* double mutants were completely bleached out (Fig. 5*D*). However, because *gbf1* and *spa1* mutants are in different ecotype backgrounds, the slight differences in bleaching effects may be attributed to such background differences. Measurement of chlorophyll contents showed dramatic reduction in accumulation of chlorophyll in *gbf1 spa1* double mutants as compare with *gbf1* or *spa1* single mutants (Fig. 5*E*).

To determine whether mutation in *SPA1* could modulate the lateral root formation in *gbf1*, we examined the root growth of *gbf1 spa1* double mutants. Examination of root growth of 16-day-old adult plants revealed that *spa1* single mutants also produced less lateral roots similar to *gbf1* mutants, and the effect was more severe in *spa1* mutants than *gbf1* (Fig. 5*F*). The number of lateral roots formed in *gbf1 spa1* double mutants was found to be between the number of lateral roots formed in *gbf1* or *spa1* single mutants at 16-day-old plants, suggesting that GBF1 and SPA1 function antagonistically in controlling the lateral root formation (Fig. 5*F*).

The Modulation of Light-inducible Gene Expression by GBF1, COP1, and SPA1—The light-mediated induction of *CAB* and *RBCS* gene expression is differentially regulated by GBF1. Whereas GBF1 acts as a positive regulator of *CAB*, it acts as a negative regulator of *RBCS* gene expression. To determine the effect of genetic interactions between *gbf1* and *cop1 or spa1* mutants on light-regulated gene expression, we monitored the induction of *CAB1* and *RBCS-1A* genes in BL by quantitative real-time PCR. For this experiment, 5-day-old dark-grown seedlings were exposed to BL for 8 h. In dark-grown seedlings, the expression of *CAB1* was found to be significantly higher in *cop1* or *spa1* mutants as compared with *gbf1* or wild-type backgrounds. Similar higher level expression was detected in corresponding double mutants (Fig. 6*A*). Consistent with the earlier results (19), the BL-mediated induction of *CAB1* was significantly reduced in *gbf1* mutants as compared with wild type (Fig. 6*A*). The higher level induction of *CAB1* in *cop1* mutants was also reduced in *gbf1 cop1* double mutants after 8-h exposure to BL, suggesting that *gbf1* and *cop1* may function antagonistically in regulating the expression of *CAB1*. On the other hand, the level of induction of *CAB1* was significantly elevated in *spa1* mutants as compared with wild type and remained about the same in *gbf1 spa1* double mutants with no detectable effect of

gbf1 mutation (Fig. 6*A*). These results demonstrate that SPA1 acts as a negative regulator of *CAB1* expression and *spa1* is epistatic to *gbf1* in BL-mediated induction of *CAB1* expression.

The level of expression of *RBCS-1A* was found to be higher in *cop1* and also in *gbf1 cop1* double mutants in dark-grown seedlings (Fig. 6*B*). However, no elevated level of expression of *RBCS-1A* was detected either in *spa1* or *gbf1 spa1* double mutants in darkness. The light-induced expression of *RBCS-1A* was significantly elevated in *gbf1 cop1* double mutants as compared with *gbf1* or *cop1* single mutants, suggesting an additive function of GBF1 and COP1 in the regulation of *RBCS-1A* gene expression in BL. Similar additive function of GBF1 and SPA1 was also detected in BL-mediated induction of *RBCS-1A* gene expression (Fig. 6*B*).

GBF1 Accumulates at a Lower Level in Dark-grown Seedlings—The stability of the regulatory proteins plays an important role in light-mediated seedling development. Earlier studies have shown that *GBF1* mRNA was present at higher level in darkness as compared with WL-grown seedlings. Furthermore, it has also been shown that the accumulation of GBF1 protein remains at the similar levels in darkness and lower intensity of WL. To further test and expand our understanding about the pattern of accumulation of GBF1 protein in wild-type background, we grew the seedlings in darkness or at various fluence rates of WL and performed immunoblot analyses. It is worth mentioning here that, although the affinity-purified antibody to GBF1 is sufficiently specific to monitor the level of GBF1 protein, it cross-reacted with a protein band (also present in *gbf1* null mutant background) that migrates just below GBF1. Furthermore, to examine whether the affinity-purified antibody of GBF1 used in this study was able to cross-react with GBF2 or GBF3 proteins, we performed Western blot analyses using purified GST-GBF1, GST-GBF2, and GST-GBF3 proteins. However, no cross-reactivity was detected (Fig. 7*E*). As shown in Fig. 7*A*, whereas the GBF1 protein accumulated to a lower level in darkness or at lower intensity of WL, the level of GBF1 protein increased at higher fluence rates of WL. To determine kinetics of accumulation of GBF1 protein, we transferred 4-day-old dark-grown seedlings to WL for various time points. GBF1 protein was detectable at lower levels in dark-grown seedlings, and the level of accumulation of the protein increased with longer exposure to WL (Fig. 7*B*). These results collectively suggest that GBF1 protein accumulates to a lower level in darkness and at lower intensity of WL, however it accumulates at higher levels at higher fluence rates of WL.

Because GBF1 is a BL-specific transcription factor, we wanted to determine whether the light-mediated accumulation of GBF1 protein is specific to a particular wavelength of light. To address this question, seedlings grown in the constant darkness or various wavelengths of light were used. As shown in Fig. 7*C*, although slightly increased levels of accumulation of GBF1 protein were detected in RL and FR, the level of accumulation was found to be maximum in WL and BL. To further test these results, we transferred dark-grown seedlings to RL, FR, or BL for various time points and monitored the GBF1 protein level. Similar to WL, GBF1 protein accumulated at higher levels in seedlings exposed to BL (Fig. 7*D*). Whereas exposure to RL showed a weak increase in the level of accumulation of GBF1 protein, there was hardly any increased level of accumulation of the protein in FR (Fig. 7*D*). Taken together, these results suggest that light-mediated accumulation of GBF1 is more prominent in BL and WL.

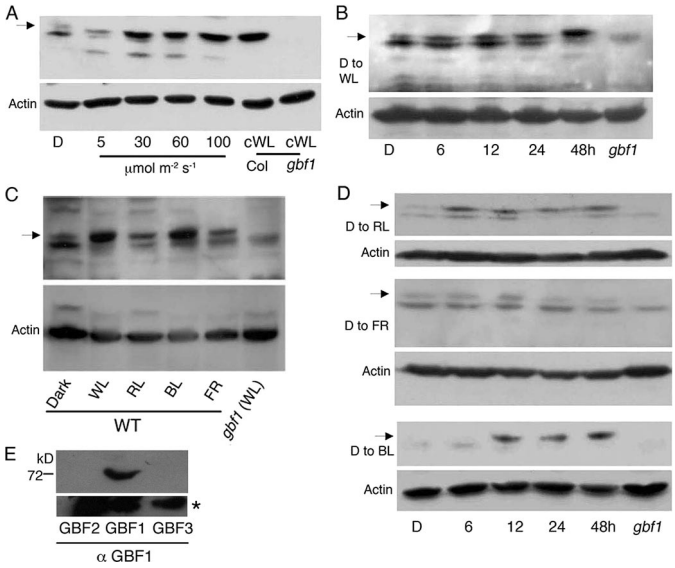

FIGURE 7. **Accumulation of GBF1 in dark- or light-grown seedlings.** Immunoblots of anti-actin (*Actin*) is shown below as loading control. The *arrow* indicates GBF1 protein band. *A*, immunoblot analyses of 4-day-old dark (*D*)-grown wild-type seedlings transferred to various intensities of WL for 24 h. *Col* and *gbf1* indicate immunoblot using 6-day-old constant WL (*cWL*: 100 μmol m^{-2} s^{-1}) grown wild-type (*Col*) or *gbf1* mutant seedlings, respectively. *B*, immunoblot analyses of 4-day-old dark (*D*)-grown wild-type seedlings transferred to WL (30 μmol m^{-2} s^{-1}) for various time points. *gbf1* indicates immunoblot using 6-day-old constant WL (30 μmol m^{-2} s^{-1})-grown *gbf1* seedlings. *C*, immunoblot analyses of 6-day-old constant dark, WL (90 μmol m^{-2} s^{-1}), RL (90 μmol m^{-2} s^{-1}), FR (80 μmol m^{-2} s^{-1}), or BL (40 μmol m^{-2} s^{-1})-grown wild-type (*Col*) seedlings. *gbf1* (*WL*) indicates immunoblot using *gbf1* mutant seedlings grown in WL (90 μmol m^{-2} s^{-1}). *D*, immunoblot analyses of 4-day-old dark (*D*)-grown wild-type seedlings transferred to RL (90 μmol m^{-2} s^{-1}), FR (80 μmol m^{-2} s^{-1}), or BL (40 μmol m^{-2} s^{-1}) for various time points. *gbf1* indicates immunoblot using 6-day-old constant RL, FR, or BL grown *gbf1* seedlings. *E*, specificity of affinity-purified GBF1 antibody. Immunoblot analysis of GST-GBF1 and GST-GBF2 and GST-GBF3 proteins. Affinity-purified GBF1 antibodies were used as primary antibody for detection. The same blot was probed with anti GST antibody to show equal loading (*star*).

Degradation of GBF1 in Dark Is Independent of COP1 and SPA1—To determine the possible roles of COP1 or SPA1 in the accumulation of GBF1 protein, we examined the level of GBF1 in *cop1* or *spa1* mutant backgrounds in dark- and light-grown conditions. As shown in Fig. 8*A*, the level of GBF1 protein was similar in *cop1*, *spa1*, and wild-type seedlings in darkness, suggesting that COP1 or SPA1 are not involved in the reduced stability of GBF1 protein in the darkness. In contrast, the level of GBF1 protein was significantly reduced in WL-grown *cop1* or *spa1* mutants as compared with wild-type seedlings (Fig. 8*B*). However, the effect of *cop1* or *spa1* mutations was not seen at lower fluence rates of WL (Fig. 8*B*). Because the accumulation of GBF1 was found to be higher in BL similar to WL, we examined whether COP1 and SPA1 were also required for the stability of GBF1 in BL. We performed immunoblot experiments using seedlings grown in BL. As shown is Fig. 8*C*, whereas there was a slight reduction (if any) in the level of GBF1 protein in *spa1* mutants, a drastic reduction in the accumulation of GBF1 was detected in *cop1* mutant backgrounds in BL. The GBF1 protein levels did not alter in *hy5* and *hyh* mutant backgrounds

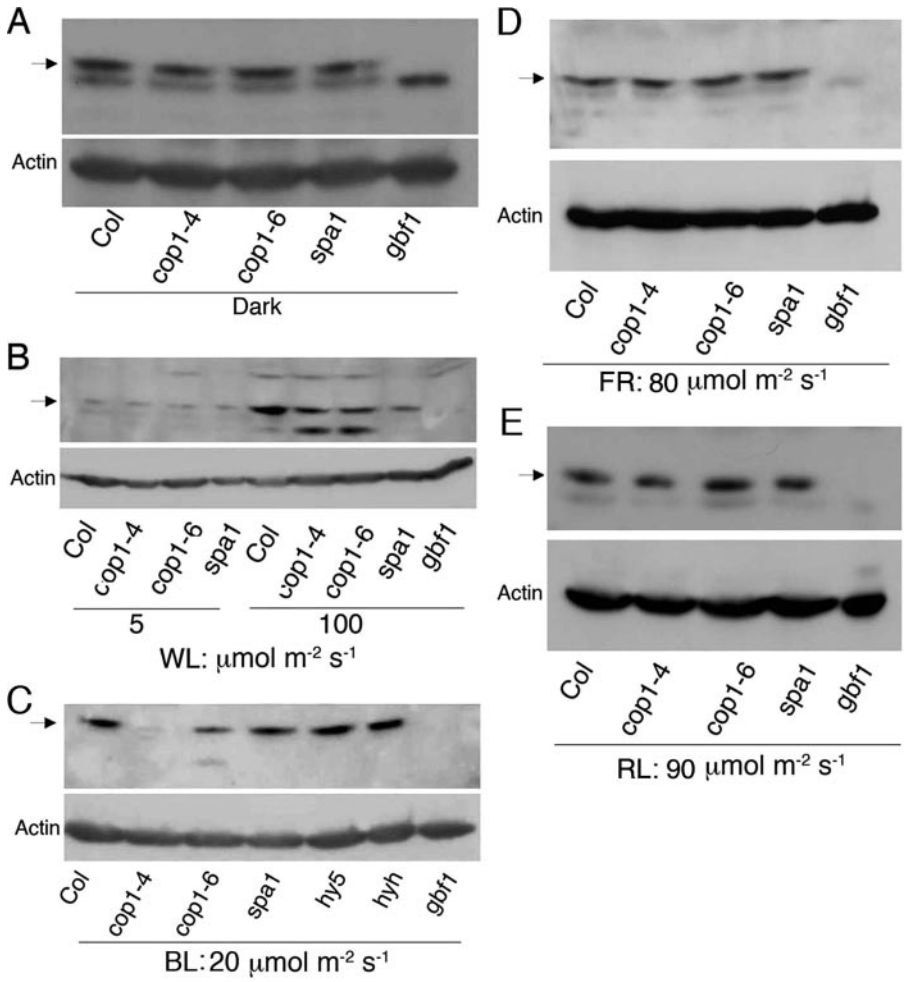

FIGURE 8. **Accumulation of GBF1 protein in *cop1* and *spa1* mutant backgrounds.** Immunoblots of anti-actin (*Actin*) is shown below as loading control. The *arrow* indicates GBF1 protein band. *A*, immunoblot using 6-day-old constant dark-grown wild-type and various mutant seedlings. *B*, immunoblot using 6-day-old constant WL (5 or 100 μmol m^{-2} s^{-1}) grown wild-type (*Col*) and various mutant seedlings. *C–E*, immunoblot using constant BL-, FR-, or RL-grown wild-type (*Col*) and various mutant seedlings, respectively.

in BL, used as controls. We also tested the level of accumulation of GBF1 protein in RL or FR in *cop1* or *spa1* mutant backgrounds. However, the level of GBF1 protein remained unaltered in *cop1* or *spa1* mutants under either RL or FR condition (Fig. 8, *D–E*). Taken together these results suggest that, whereas COP1 and SPA1 are required to maintain the higher level of accumulation of GBF1 in WL, COP1 is predominantly involved in the accumulation of GBF1 protein in BL.

GBF1 Is Degraded through a 26 S Proteasome-dependent Pathway in Dark—To examine whether the lower level accumulation of GBF1 in dark-grown seedlings was due to GBF1 degradation mediated by the 26 S proteasome, we tested the effects of proteasome inhibitors, MG132, MG115, and *N*-acetyl-leucyl-leucyl-norleucinal, on GBF1 protein accumulation. Four-day-old dark-grown wild-type seedlings were treated with proteasome inhibitors or mock treated with 0.1% DMSO for 12 h, and total protein was extracted and used for immunoblot analysis. As shown in Fig. 9*A*, treatment with proteasome inhibitors significantly increased GBF1 protein accumulation in dark-grown seedlings. Next, we carried out a time-course experiment to determine the degradation kinetics of GBF1 protein in dark-grown seedlings. For this experiment, 5-day-old dark-grown wild-type or *cop1* mutant seedlings were treated with MG132 or mock treated with 0.1% DMSO for 12 h. The seedlings were then washed in the dark and incubated in darkness for different time points. Total protein was extracted and subjected to immunoblot analysis. As shown in Fig. 9 (*B–D*), significantly higher levels of GBF1 protein were detected up to 6 h after the treatment of MG132 as compared with DMSO treatment both in wild-type and *cop1* mutants. Furthermore, the level of GBF1 protein declined similarly at 12 h either in wild-type or *cop1* mutant background. These results demonstrate that GBF1 protein is subject to 26 S proteasome-mediated proteolysis in dark-grown seedlings. These results, taken together with the results in Fig. 8*A*, further demonstrate that the 26 S proteasome-mediated degradation of GBF1 in the dark is indeed independent of COP1.

To determine whether lower level accumulation of GBF1 protein at lower fluence rates of WL (Figs. 7*A* and 8*B*) is due to GBF1 degradation mediated by the 26 S proteasome, we performed similar experiments as described above. However, as shown in Fig. 9*E*, the level of GBF1 protein remained at the similar levels either in DMSO- or MG132-treated seedlings, suggesting that reduced accumulation of GBF1 at lower fluences of WL is not due to 26 S proteasome-mediated proteolysis.

GBF1 Physically Interacts with COP1—To determine whether the requirement of COP1 for the optimum level of accumulation of GBF1 protein is through direct physical interactions between these two proteins, we carried out protein-protein interaction studies. To examine such possible physical interactions, first an *in vitro* binding experiment was performed. As shown in Fig. 10*A*, the amount of COP1 retained by GST-GBF1 beads were significantly higher than the background level of COP1 retained by the control GST beads. Because equal amounts of GST-GBF1 or GST were used in the binding experiments, these results indicate a direct protein-protein interaction between GBF1 and COP1 *in vitro*. To further substantiate the observed *in vitro* COP1 and GBF1 interaction, a yeast two-hybrid protein-protein interaction assay was carried out. As shown in Fig. 10*B*, chimeric fusion protein of the GAL4 activation domain and GBF1 (AD-GBF1) or HY5 (AD-HY5; used as a control) activated transcription of the lacZ reporter gene in the presence of GAL4 DNA-binding domain-COP1 fusion protein (BD-COP1) but not with GAL4 DNA binding domain (BD) alone, suggesting a direct protein-protein

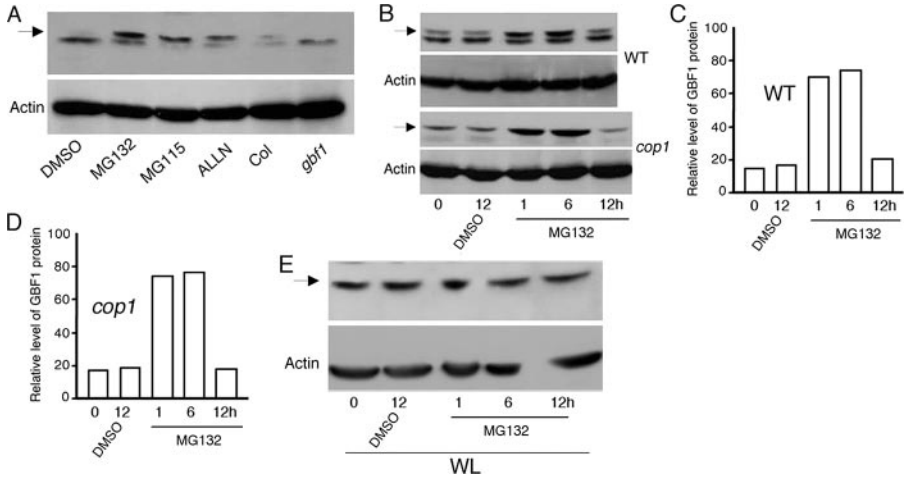

FIGURE 9. **Degradation of GBF1 protein in darkness by COP1-independent proteasomal pathway.** Immunoblots of anti-actin (*Actin*) is shown below as loading control. The *arrow* indicates GBF1 protein band. *A*, 5-day-old dark-grown wild-type seedlings were treated with MG132, MG115, or *N*-acetyl-leucyl-leucyl-norleucinal or mock treated with 0.1% DMSO for 12 h. *Col* and *gbf1* indicate wild-type and *gbf1* mutant seedlings without treatments. Total protein was extracted and subjected to immunoblot analysis. *B*, 5-day-old dark-grown wild-type (*WT*) or *cop1-4* mutant seedlings were treated with MG132 or mock treated with 0.1% DMSO for 12 h. The seedlings were then thoroughly washed in the dark and incubated in darkness for different time points. Total protein was extracted and subjected to immunoblot analysis. *C*, quantification and normalization (by Fluor-S-Multilmager (Bio-Rad)) of the protein levels with the actin band as shown in *B* (*WT*). *D*, quantification and normalization (by Fluor-S-Multilmager (Bio-Rad)) of the protein levels with the actin band as shown in *B* (*cop1*). *E*, 5-day-old WL-grown wild-type seedlings were treated with MG132 or mock treated with 0.1% DMSO for 12 h. The seedlings were then thoroughly washed and incubated in WL for different time points. Total protein was extracted and subjected to immunoblot analysis.

interaction between COP1 and GBF1 in yeast cells. Finally, we performed an *in vitro* coimmunoprecipitation experiment to further substantiate the physical interaction between GBF1 and COP1 proteins. As shown in Fig. 10*C*, GBF1 interacted with COP1 in an *in vitro* interaction assays using recombinant proteins. Approximately 11% of the added COP1 protein was coimmunoprecipitated with GST-GBF1, whereas <0.8% of the added COP1 was able to bind to GST alone. Taken together, these results demonstrate that GBF1 can physically interact with COP1.

DISCUSSION

In this study, we establish the genetic and molecular relationships of a BL-specific transcription factor, GBF1, with two well characterized negative regulators of light signaling, COP1 and SPA1 in photomorphogenic growth and light-regulated gene expression. This study further demonstrates that GBF1 protein is less abundant in the dark-grown seedlings and is degraded by a proteasome-mediated pathway independent of COP1 and SPA1. On the other hand, COP1 physically interacts with GBF1 and is required for the optimum accumulation of GBF1 protein in light-grown seedlings (Fig. 10*D*).

The Integrated Functions of GBF1, COP1, and SPA1 in Photomorphogenic Growth and Light-regulated Gene Expression—The double mutant analyses reveal that GBF1 and COP1 function redundantly in the dark to suppress photomorphogenic growth. The enhanced inhibition of hypocotyl elongation displayed by *gbf1* mutants in WL requires functional COP1, however not in BL (Fig. 1). Thus, whereas GBF1 requires COP1 function in darkness to suppress photomorphogenic growth, these two proteins are likely to function in parallel pathways and in an additive manner to suppress photomorphogenic growth in BL. GBF1 and SPA1 appear to act as independent negative regulators in WL-mediated inhibition of hypocotyls elongation (Fig. 4). GBF1 acts as a positive regulator of cotyledon expansion and the expanded cotyledon phenotype of *cop1-4* mutants was completely suppressed in *gbf1 cop1*double mutants in BL. Therefore, GBF1 and COP1 act antagonistically in BL-mediated cotyledon expansion. On the other hand, *gbf1 spa1* double mutants exhibit similar cotyledon expansion as *spa1* single mutants suggesting that the positive regulatory function of GBF1 requires functional SPA1.

The differential regulation of GBF1 in *CAB1* and *RBCS-1A* gene expression is almost nullified in *gbf1 cop1* and *gbf1 spa1* double mutants, because both the genes are expressed at higher levels in double mutant backgrounds (Fig. 6). However, the light-mediated enhanced expression of *CAB1* in *cop1* mutants was significantly reduced in *gbf1 cop1* double mutants suggesting that COP1 and GBF1 might play antagonistic roles in the regulation of *CAB1* gene expression. The expression of *CAB1* was derepressed in the dark in *spa1* mutants, however no such effect of *spa1* mutation was detected on *RBCS-1A* gene expression. The higher level expression of *RBCS-1A* in *cop1* or *gbf1* mutants was further enhanced in *gbf1 cop1* and *gbf1 spa1* double mutants. Therefore, GBF1 functions in an additive manner with COP1 or SPA1, and thus likely acts in parallel pathways to regulate the expression of *RBCS-1A*.

Accumulation of GBF1 Depends on the Presence of COP1 and SPA1 in Light-grown Seedlings—Light-regulated shuttling of COP1 between the nucleus and cytoplasm is an important regulatory mechanism of light-mediated seedling development (3, 27). COP1 degrades several photomorphogenesis promoting factors in the dark to suppress photomorphogenic growth in the darkness. SPA1 is an associated factor of COP1 for the degradation of some of these regulatory proteins such as HY5, LAF1, and HFR1 (28, 29, 33–36). On the contrary, COP1 positively regulates PIF3 accumulation in darkness (48).

Our results demonstrate that, whereas COP1 and SPA1 are not associated with the stability of GBF1 protein in the dark, functional COP1 protein is required to maintain the stability of GBF1 protein in WL and BL. This study further demonstrates that GBF1 physically interacts with COP1, suggesting a direct role of COP1 in maintaining the stability of GBF1 protein. GBF1 plays both negative and positive regulatory roles in *Arabidopsis* seedling development. Higher level accumulation of GBF1 results in elongated hypocotyls, however more expanded cotyledons (19). Therefore, a fine-controlled level of GBF1 is likely to be essential to obtain light-mediated optimum photo-

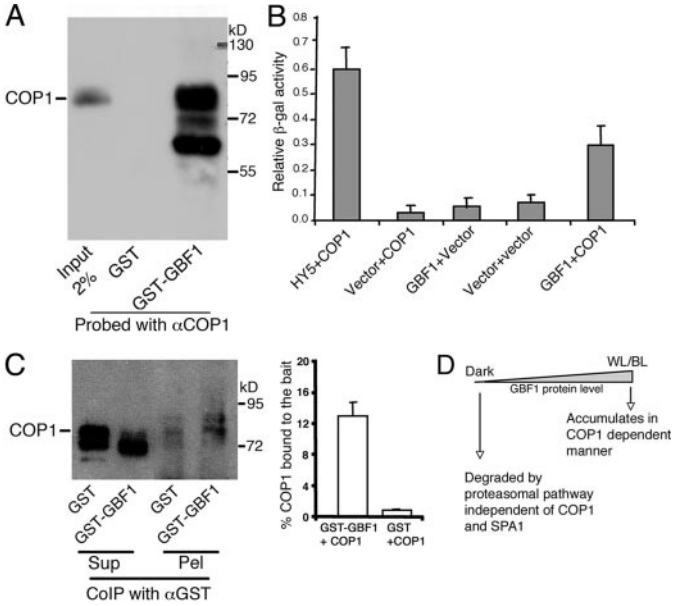

FIGURE 10. **GBF1 and COP1 physically interact with each other.** *A, in vitro* binding of GBF1 and COP1: ~5 μg of GST or GST-GBF1 was bound to the glutathione-Sepharose 4B beads, washed, and incubated with COP1–6His (5 μg). Beads were washed and fractionated in 10% SDS-PAGE. The blot was probed with anti-COP1 antibodies. *B*, yeast two-hybrid interactions of GBF1 and COP1: The AD-GBF1 or AD-HY5 (as control) and BD-COP1 constructs were co-transformed into yeast strain AH109. The protein-protein interactions were examined by β-galactosidase assays. The relative β-galactosidase activities were calculated according to Clontech instructions. The *error bars* indicate standard errors ($n = 3$). *C, in vitro* coimmunoprecipitation of COP1 by GBF1: GST-GBF1 or GST was incubated with recombinant COP1 protein (COP1–6His) and coimmunoprecipitated with anti-GST antibodies. Supernatant and pellet fractions were fractionated in SDS-PAGE, blotted, and probed with anti-COP1 antibodies. Quantification of the fractions (by Fluor-S-Multi-Imager (Bio-Rad)) of COP1 that were coimmunoprecipitated by GST or GST-GBF1 are shown in the *graph* (*right side*). *Error bars* indicate standard error of the mean of two replicate experiments. *D*, a working model describes the higher level accumulation of GBF1 protein in WL and BL. GBF1 protein is degraded by proteasome-mediated pathway in the dark, independent of COP1 and SPA1, and it accumulates in WL and BL in a COP1-dependent manner.

morphogenic growth. Because GBF1 protein accumulates at higher levels with higher fluence rates of WL in a COP1-dependent manner, it could be envisioned that light-induced translocation of COP1 between nucleus and cytosol might be a potential mechanism to control the level of GBF1 protein and thereby its function in photomorphogenesis.

The mechanism of differential regulatory function of GBF1, COP1, and SPA1 remains to be elucidated. One plausible explanation of differential regulatory roles of COP1 and SPA1 might be that they differentially degrade or stabilize the proteins with positive or negative regulatory functions (for example HY5 and PIF3) and thereby differentially regulate the expression of the target genes. GBF1, on the other hand, might function either as a transcriptional activator or repressor, depending on the promoter determinants of the target genes. Alternatively, it could be envisioned that hetero-dimerization of GBF1 with other bZIP proteins (such as HY5 or HYH) might be a potential mechanism to generate positive and negative regulators, which in turn play positive or negative regulatory roles in signaling cascades. In either case, further study is required to test the possibility.

Acknowledgments—We are thankful to Peter H. Quail and X. W. Deng for spa1 and cop1 seeds, respectively.

REFERENCES

1. Chen, M., Chory, J., and Fankhauser, C. (2004) *Annu. Rev. Genet.* **38,** 87–117
2. Huq, E., and Quail, P. H. (2005) in *Handbook of Photosensory Receptors* (Briggs, W. R., and Spudich, J. L., eds) pp. 151–170, Wiley VCH, Weinheim, Germany
3. Jiao, Y., Lau, O. S., and Deng, X.-W. (2007) *Nat. Rev.* **8,** 217–230
4. Cashmore, A. R., Jarillo, J. A., Wu, Y. J., and Liu, D. (1999) *Science* **284,** 760–765
5. Lin, C. (2002) *Plant Cell* **5,** S207–S225
6. Schepens, I., Duek, P., and Fankhauser, C. (2004) *Curr. Opin. Plant Biol.* **7,** 564–569
7. Briggs, W. R., and Christie, J. M. (2002) *Trends Plant Sci.* **7,** 204–210
8. Kircher, S., Gil, P., Kozma-Bognar, L., Fejes, E., Speth, V., Husselstein, T., Bury, E., Àdam, É., Schäfer, E., and Nagy, F. (2002) *Plant Cell* **14,** 1541–1555
9. Nagy, F., and Schafer, E. (2002) *Annu. Rev. Plant Biol.* **53,** 329–355
10. Kleine, T., Lockhart, P., and Batschauer, A. (2003) *Plant J.* **35,** 93–103
11. Oyama, T., Shimura, Y., and Okada, K. (1997) *Genes Dev.* **11,** 2983–2995
12. Ang, L.-H., Chattopadhyay, S., Wei, N., Oyama, T., Okada, K, Batschauer, A., and Deng, X.-W. (1998) *Mol. Cell* **1,** 213–222
13. Chattopadhyay, S., Ang, L. H., Puente, P., Deng, X. W., and Wei, N. (1998) *Plant Cell* **10,** 673–683
14. Guo, H., Mocker, T., Duong, H., and Lin, C. (2001) *Science* **291,** 487–490
15. Holm, M., Ma, L.-G., Qn, L.-J., and Deng, X. W. (2002) *Genes Dev.* **16,** 1247–1259
16. Moller, S. G., Kim, Y.-S., Kunkel, T., and Chua, N.-H. (2003). *Plant Cell* **15,** 1111–1119
17. Ward, J. M., Cufr, C. A., Denzel, M. A., and Neff, M. M. (2005) *Plant Cell* **17,** 475–485
18. Yadav, V., Mallappa, C., Gangappa, S. N., Bhatia, S., and Chattopadhyay, S. (2005) *Plant Cell* **17,** 1953–1966
19. Mallappa, C., Yadav, V., Negi, P., and Chattopadhyay, S. (2006) *J. Biol. Chem.* **281,** 22190–22199
20. Nagatani, A., Reed, J. W., and Chory, J. (1993) *Plant Physiol.* **102,** 269–277
21. Whitelam, G. C., Johnson, E., Peng, J., Carol, P., Anderson, M. L., Cowl, J. S., and Harberd, N. P. (1993) *Plant Cell* **5,** 757–768
22. Neff, M. M., Fanhauser, C., and Chory, J. (2000) *Genes Dev.* **14,** 257–271
23. Wang, H., and Deng, X. W. (2004) in *The Arabidopsis Book* (Somerville, C. R., and Meyerowitz, E. M., eds) pp. 1–23, American Society of Plant Physiologists, Rockville, MD
24. Tepperman, J. M., Zhu, T., Chang, H. S., Wang, X., and Quail, P. H. (2001) *Proc. Natl. Acad. Sci. U. S. A.* **98,** 9437–9442
25. Ma, L., Li, J., Qu, L., Hager, J., Chen, Z., Zhao, H., and Deng, X. W. (2001) *Plant Cell* **13,** 2589–2607
26. Wei, N., and Deng, X. W. (1999) *Trends Genet.* **15,** 98–103
27. Osterlund, M. T., Hardtke, C. S., Wei, N., and Deng, X. W. (2000) *Nature* **405,** 462–466
28. Seo, H. S., Watanabe, E., Tokotomi, S., Nagatani, A., and Chua, N. H. (2004) *Genes Dev.* **18,** 617–622
29. Jang, I. C., Yang, J. Y., Seo, H. S., and Chua, N. H. (2005) *Genes Dev.* **19,** 593–602
30. Yang, J., Lin, R., Sullivan, J., Hoecker, U., Liu, B., Xu, L., Deng, X. W., and Wang, H. (2005) *Plant Cell* **17,** 804–821
31. McNellis, T. W., Von Arnim, A. G., Araki, T., Komeda, Y., Misera, S., and Deng, X. W. (1994) *Plant Cell* **6,** 487–500
32. Deng, X. W., and Quail, P. H. (1999) *Semin. Cell & Dev. Biol.* **10,** 121–129
33. Hoecker, U., Tepperman, J. M., and Quail, P. H. (1999) *Science* **284,** 496–499
34. Saijo, Y., Sullivan, J. A., Wang, H., Yang, J., Shen, Y., Rubio, V., Ma, L., Hoecker, U., and Deng, X. W. (2003) *Genes Dev.* **17,** 2642–2647
35. Seo, H. S., Yang, J. Y., Ishikawa, M., Bole, C., Ballesteros, M. L., and Chua, N.-H. (2003) *Nature* **423,** 995–999

36. Laubinger, S., Fittingoff, K., and Hoecker, U. (2004) *Plant Cell* **16,** 2293–2306
37. Yang, J., Lin, R., Roecker, U., Liu, B., Xu, L., and Wang, H. (2005) *Plant J.* **43,** 131–141
38. Baumgardt, R. L., Oliverio, K. A., Casal, J. J., and Hoecker, U. (2002) *Planta* **215,** 745–753
39. Fittinghoff, K., Laubinger, S., Nixdorf, M., Fackendahl, P., Baumgardt, R. L., Batschauer, A., and Hoecker, U. (2006) *Plant J.* **47,** 577–590
40. Schindler, U., Menkens, A. E., Beckmann, H., Ecker, J. R., and Cashmore, A. R. (1992) *EMBO J.* **11,** 1261–1273
41. Foster, R., Izawa, T., and Chua, N.-H. (1994) *FASEB J.* **8,** 192–200
42. Menkens, A. E., Schindler, U., and Cashmore, A. R. (1995) *Trends Biochem. Sci.* **20,** 506–510
43. Terzaghi, W. B., and Cashmore A. R. (1995) *Annu. Rev. Plant Physiol. Plant Mol. Biol.* **46,** 445–474
44. Puente, P., Wei, N., and Deng, X. W. (1996) *EMBO J.* **15,** 3732–3743
45. Chattopadhyay, S., Puente, P., Deng, X.-W., and Wei, N. (1998) *Plant J.* **15,** 69–77
46. Terzaghi, W. B., Bertekap, R. L., Jr., and Cashmore, A. R. (1997) *Plant J.* **11,** 967–982
47. Ang, L. H., and Deng, X.-W. (1994) *Plant Cell* **6,** 613–628
48. Bauer, D., Viczián, A., Kircher, S., Nobis, T., Nitschke, R., Kunkel, T., Panigrahi, K. C., Adám, E., Fejes, E., Schäfer, E., and Nagy, F. (2004) *Plant Cell* **16,** 1433–1445